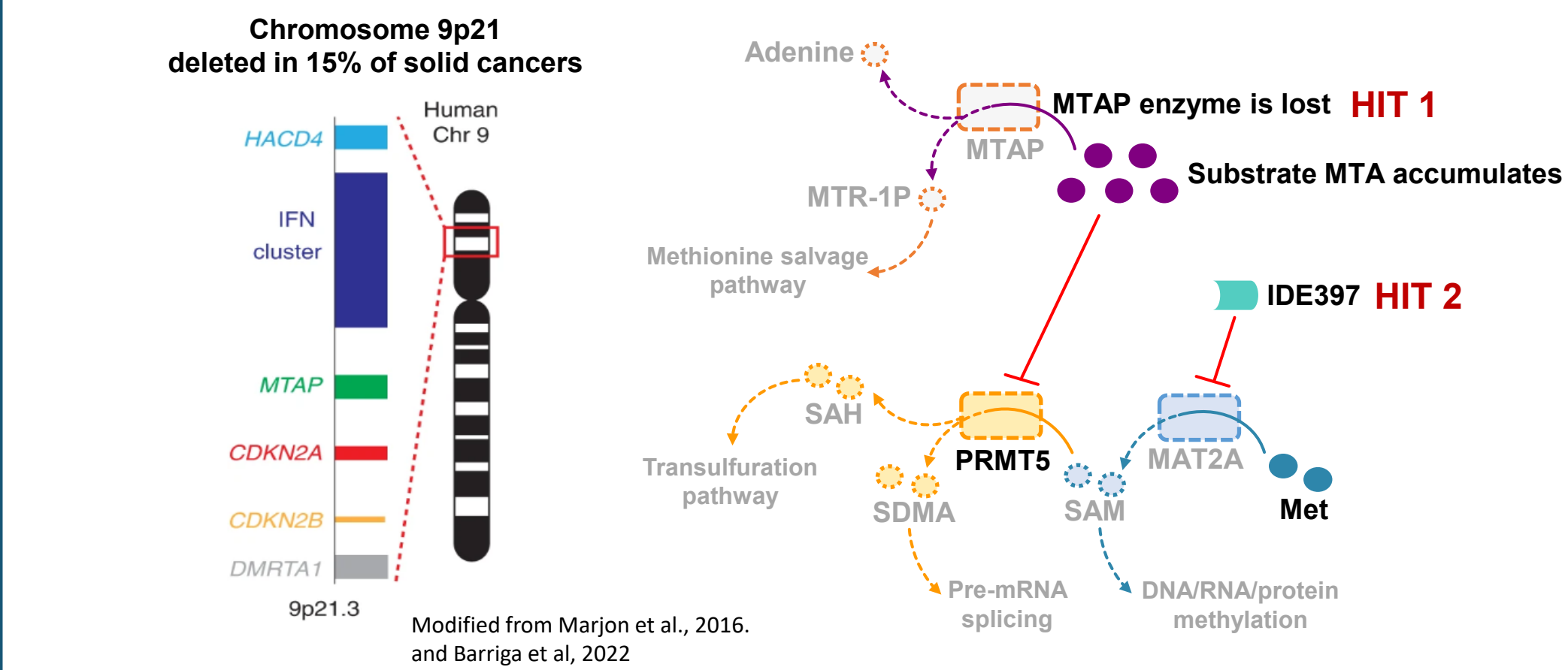


Introduction

Deletion of *MTAP* confers targetable vulnerabilities in ~15% of all solid tumors



Methylthioadenosine phosphorylase (MTAP) is co-deleted with the tumor suppressor *CDKN2A* in approximately 15% of solid tumors. This often causes an accumulation of MTA and creates a dependency on methionine adenosyltransferase 2A (MAT2A) production of S-adenosyl methionine (SAM), the primary methyl donor for methyltransferase reactions in cells. We developed IDE397, a potent small molecule inhibitor of MAT2A, to selectively exploit this synthetic lethal vulnerability in *MTAP*^{-/-} tumors. Evaluation of IDE397 efficacy across a panel of *MTAP*^{-/-} PDX models revealed consistent tumor growth inhibition across diverse lineages, with enrichment of tumor regressions in a subset of tumor types. To further enhance the efficacy of IDE397 within and among indications, we sought to identify mechanism-based combination partners. A three-pronged approach was employed that dovetailed molecular profiling of IDE397 drug effects *in vivo*; chemogenomic evaluation of selective vulnerabilities in *MTAP*^{-/-} cell lines across the CCLE; and high-throughput drug combination screens.

Objectives

- Define molecular associations that specify sensitivity to IDE397
- Annotate the landscape of biological systems that represent cellular vulnerabilities conferred by MTAP deficiency
- Isolate the common drug effect (IDE397) on tumor cell behavior across diverse PDX models
- Profile a diverse library of drugs and tool compounds in IDE397 synergy screens
- Integrate these observations to prioritize promising drug combination partners and evaluate performance *in vivo*

Conclusion

The enrichment of tumor regressions in a subset of PDX models suggests that *MTAP* deletion is necessary but not sufficient for a maximal antitumor response to MAT2A pathway inhibition. This context-dependent response relationship may be a consequence of model-dependent pressure on splicing fidelity and MTA accumulation (see accompanying poster #1644). However, our collective observations indicate that exposure to IDE397 can install mechanistic vulnerabilities, selectively in *MTAP*-deficient tumors, that can be exploited by appropriate combination agents to deliver antitumor benefit beyond that observed in the single agent setting. The mechanistic underpinnings of the drug synergy pairs shown here appear to be the product of targeting multiple nodes within the *MTAP*/*MAT2A*/*PRMT5* network. Of note, IDE397 can generate cell states in *MTAP*^{-/-} tumor cells that are selectively vulnerable to approved chemotherapies and targeted therapies. This chemically-conferred synthetic lethality paradigm, if translatable, suggests MAT2A inhibitors have broad potential as a backbone therapy in *MTAP*-deficient tumors.

Acknowledgements

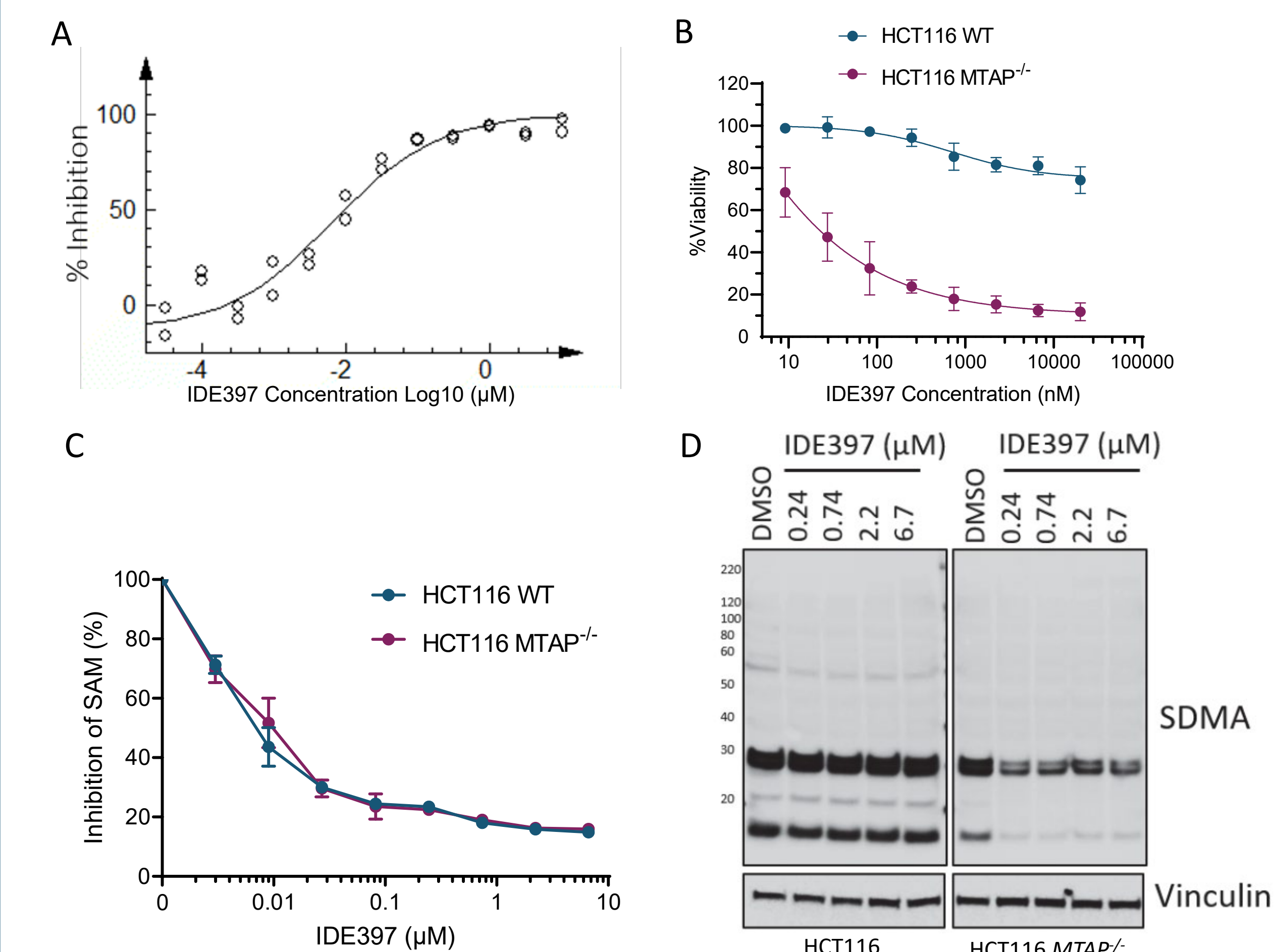
We are thankful for valuable contributions from Dr. Christian Frey, Dr. Jeanne Quirir, Dr. Neil Bhola, Atieh Givmanesh, and John Faulhaber. We are grateful to our CRO partners Horizon Discovery, Eurofins, DepMap Consortium, and HudsonAlpha Discovery.

References

- Barriga FM, et al. Nat Cancer. 2022 Nov;3(11):1367-1385.
- Marjon K, et al. Cell Rep. 2016 Apr 19;15(3):574-587.
- Korotkevich G, et al. bioRxiv; DOI: 10.1101/060012.
- Ritchie ME, et al. Nucleic Acids Res. 2015 Apr 20;43(7):e47

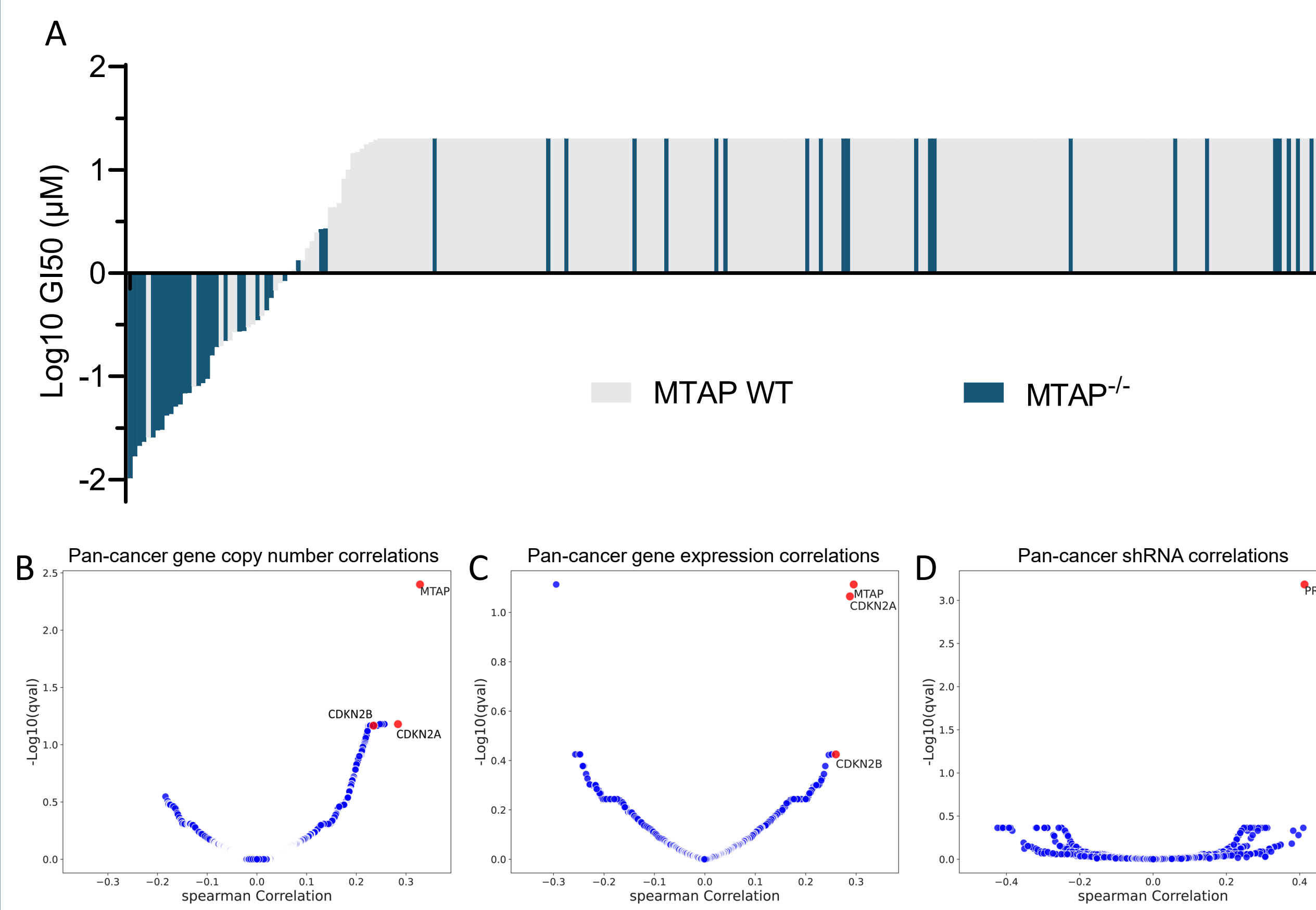
Results

Figure 1. IDE397 is a potent inhibitor of MAT2A and is selective for *MTAP* deletion



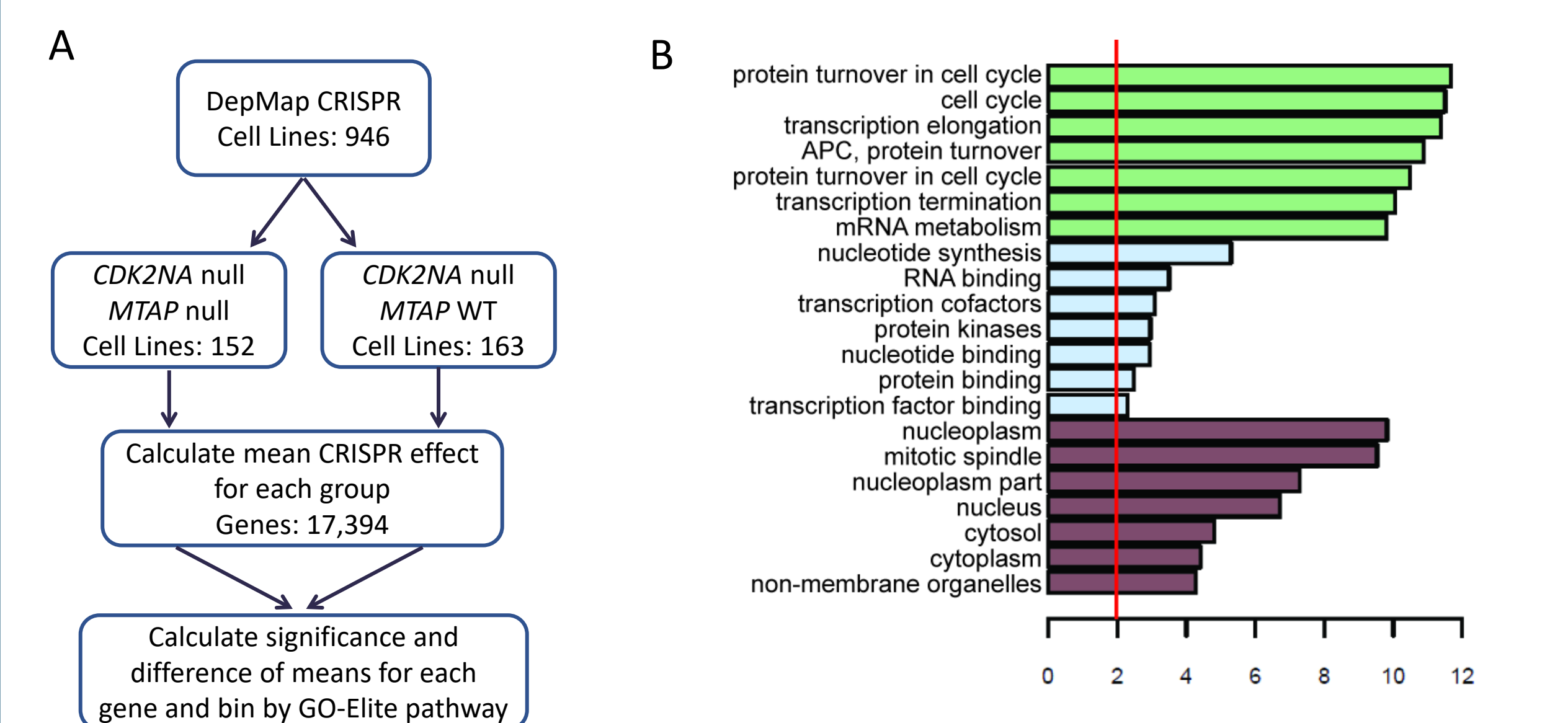
A) *In vitro* biochemical MAT2A activity assay shows potent inhibition by IDE397. B) IDE397 selectively inhibits proliferation of HCT116 *MTAP*^{-/-} compared the parental HCT116 line expressing MTAP. C) IDE397 shows equivalent inhibition of cellular SAM levels regardless of MTAP status in HCT116 cells. D) Protein symmetric di-methylation (SDMA) is selectively inhibited in HCT116 *MTAP*^{-/-} cells upon IDE397 treatment.

Figure 2. IDE397 displays a highly selective cell activity profile that correlates with 9p21.3 loss and *PRMT5* dependency



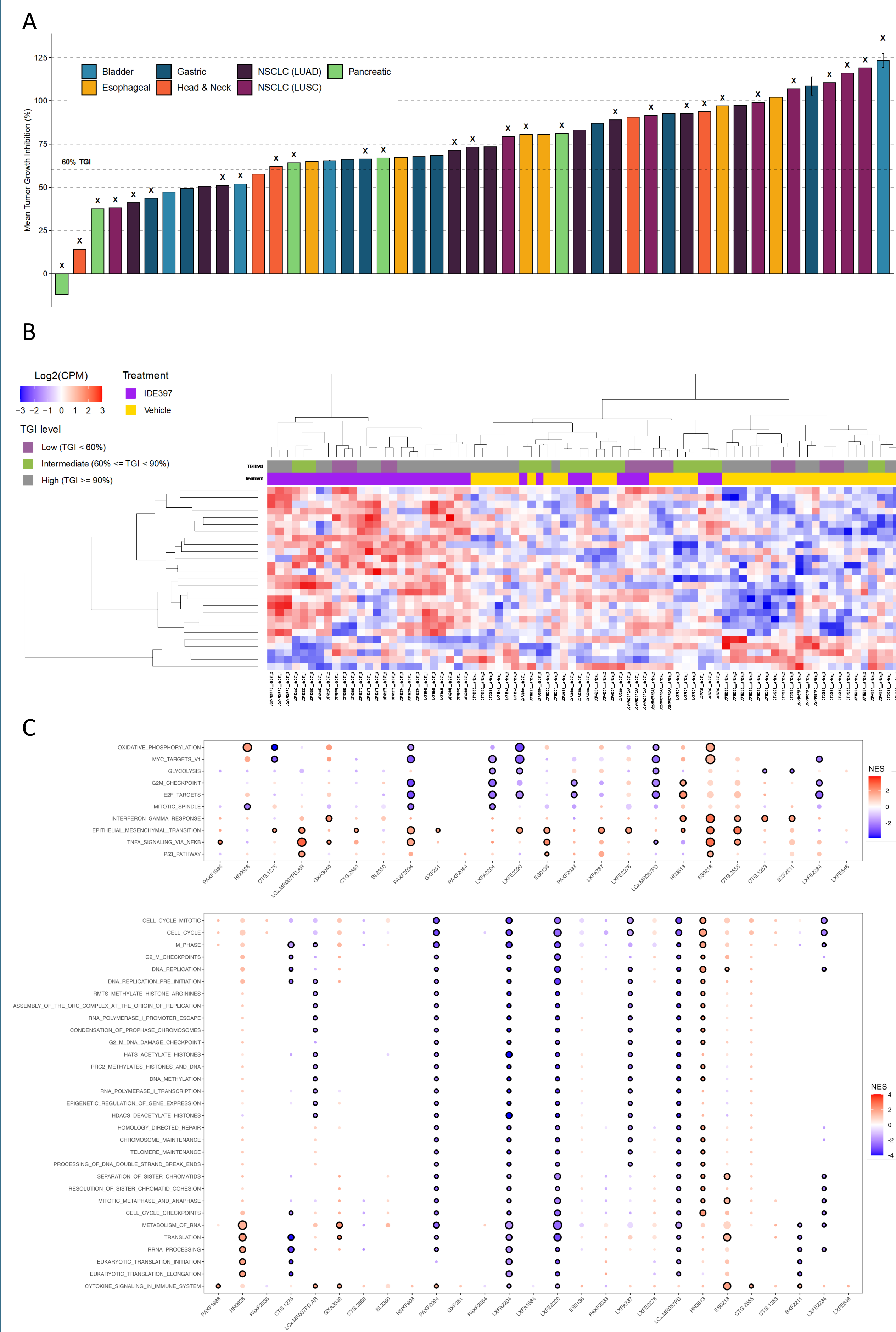
A) Waterfall plot of IDE397 GI50 values across a 263-cell line panel consisting of *MTAP*-deleted (blue) and wildtype (grey) cells representing a diversity of indications. B) Volcano plot of univariate correlation of gene copy number vs IDE397 Log10(GI50) across all 263 cell lines regardless of *MTAP* status. *MTAP*, *CDKN2A*, and *CDKN2B* are among the most strongly correlated associations. C) Corresponding volcano plot of gene expression vs IDE397. *MTAP*, *CDKN2A*, and *CDKN2B* are the most highly correlated with IDE397-sensitivity. D) Corresponding volcano plot of Achilles shRNA Gene Effect vs IDE397. *PRMT5* knockdown is the most strongly correlated with IDE397 sensitivity.

Figure 3. *MTAP* loss is associated with enhanced dependency on the fidelity of mitotic regulation, DNA/RNA metabolism, and transcription



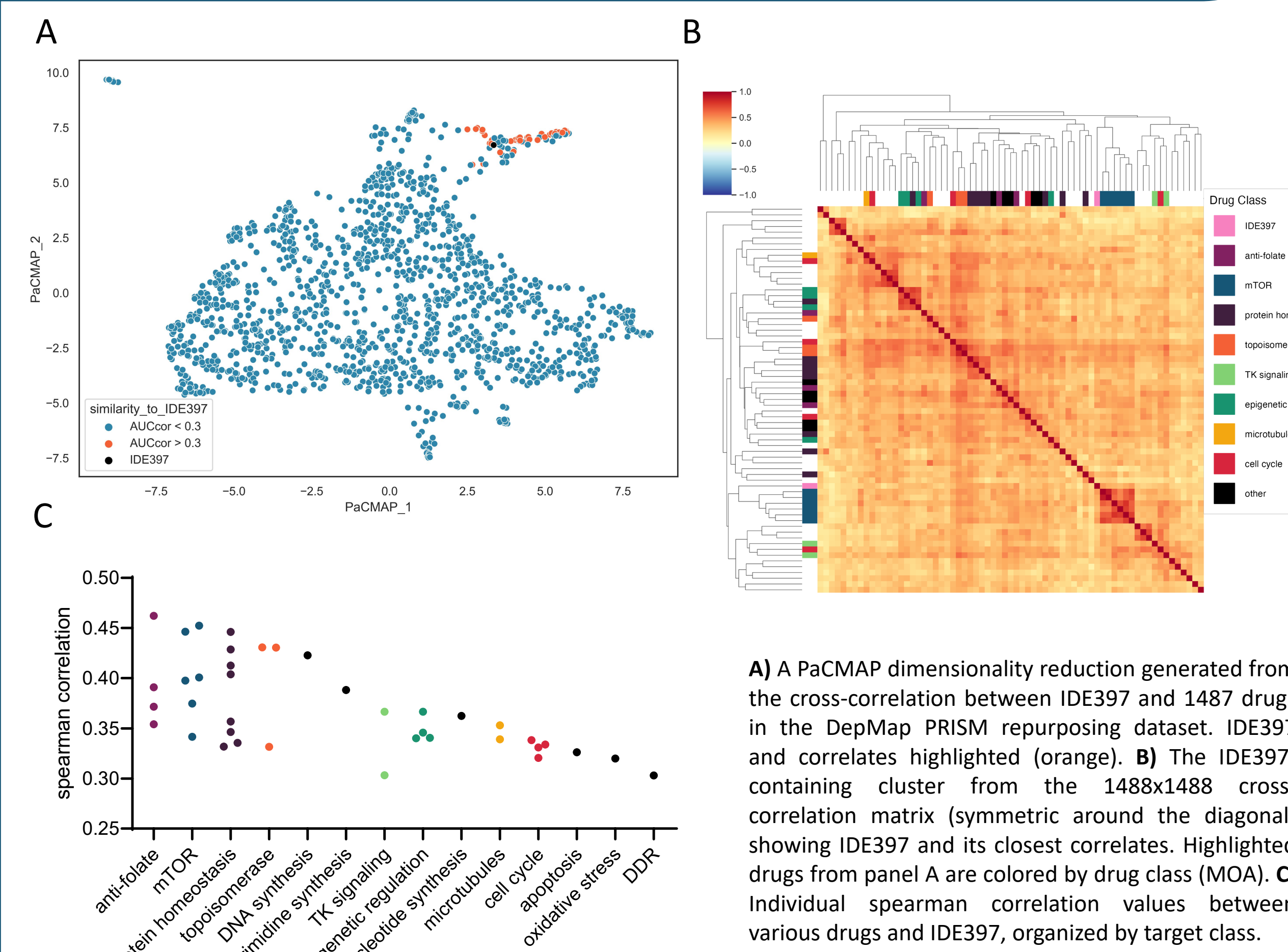
A) Schematic of workflow. Cell line CRISPR data from DepMap was used to compare *MTAP* null vs WT cells in a *CDKN2A* null context to isolate the effects of *MTAP* deletion itself. The CRISPR effects on viability were then compared between *MTAP* null and WT. B) Plot of GO-Elite group effects showing high dependence in *MTAP* null cells. Cell cycle regulation, transcription, RNA processing, protein homeostasis, and mitotic spindle regulation are among most highly correlated dependencies.

Figure 4. IDE397 perturbs the fidelity of expression networks participating in mitosis, DNA/RNA metabolism and transcription in *MTAP*-deleted PDX tumors



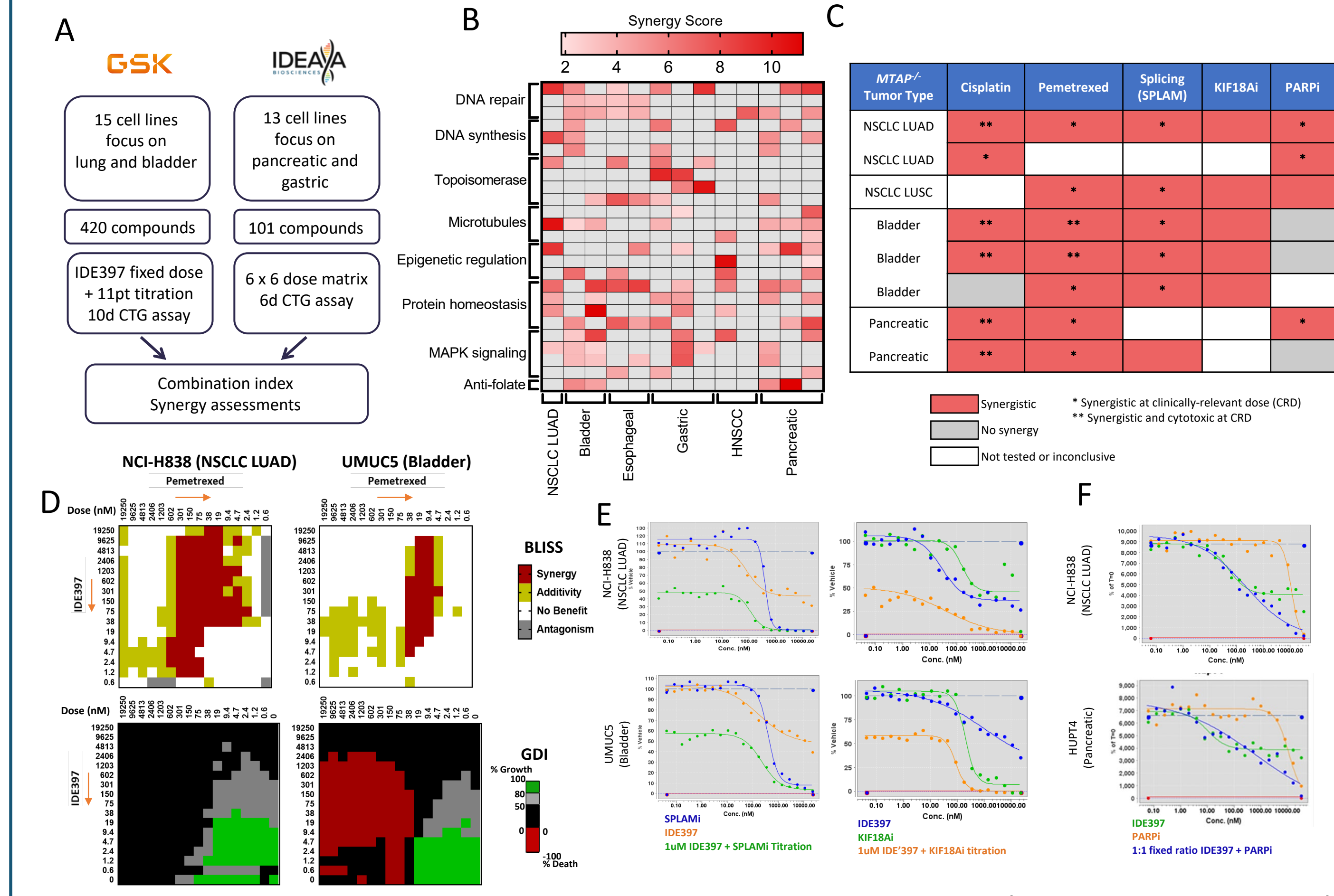
A) 47 *MTAP*-deleted PDX models were evaluated for anti-tumor response. IDE397 or vehicle was administered at 30 mg/kg/day (n=5/gp). Mean TGI was calculated from final and initial tumor volume. Tumor regression >100% TGI. Bars are colored by tumor type and samples profiled for expression analysis at the end of study via RNAseq are marked with an "x". RNAseq was performed from whole tumor lysate at study termination (n=3/gp). B) Heatmap with 2-way unsupervised hierarchical clustering of 27 NSCLC models and the significantly differentially expressed genes (FDR<0.05) between treated vs control groups. Annotation bar shows treatment status and TGI level for each sample. C) GSEA on curated, non-redundant gene sets in the MsigDB Hallmark (above) and C2 Reactome (below) collections across all NSCLC models. Dots are colored by Normalized Enrichment Score and sized based on the size of the Leading Edge of the enrichment. Dots surrounded by a black border are FDR significant (<0.05). Differential Expression profiled using limma, Enrichment analysis conducted using the R fgsea package with genes ranked by the formula $-\log_2(\text{FC} \times -\log_{10}(p))$.

Figure 5. Extensive chemical profiling reveals associations between IDE397 and compounds that perturb biological systems aligned with both *MTAP* deficiency and the consensus IDE397 drug effect in *MTAP* deficient tumors



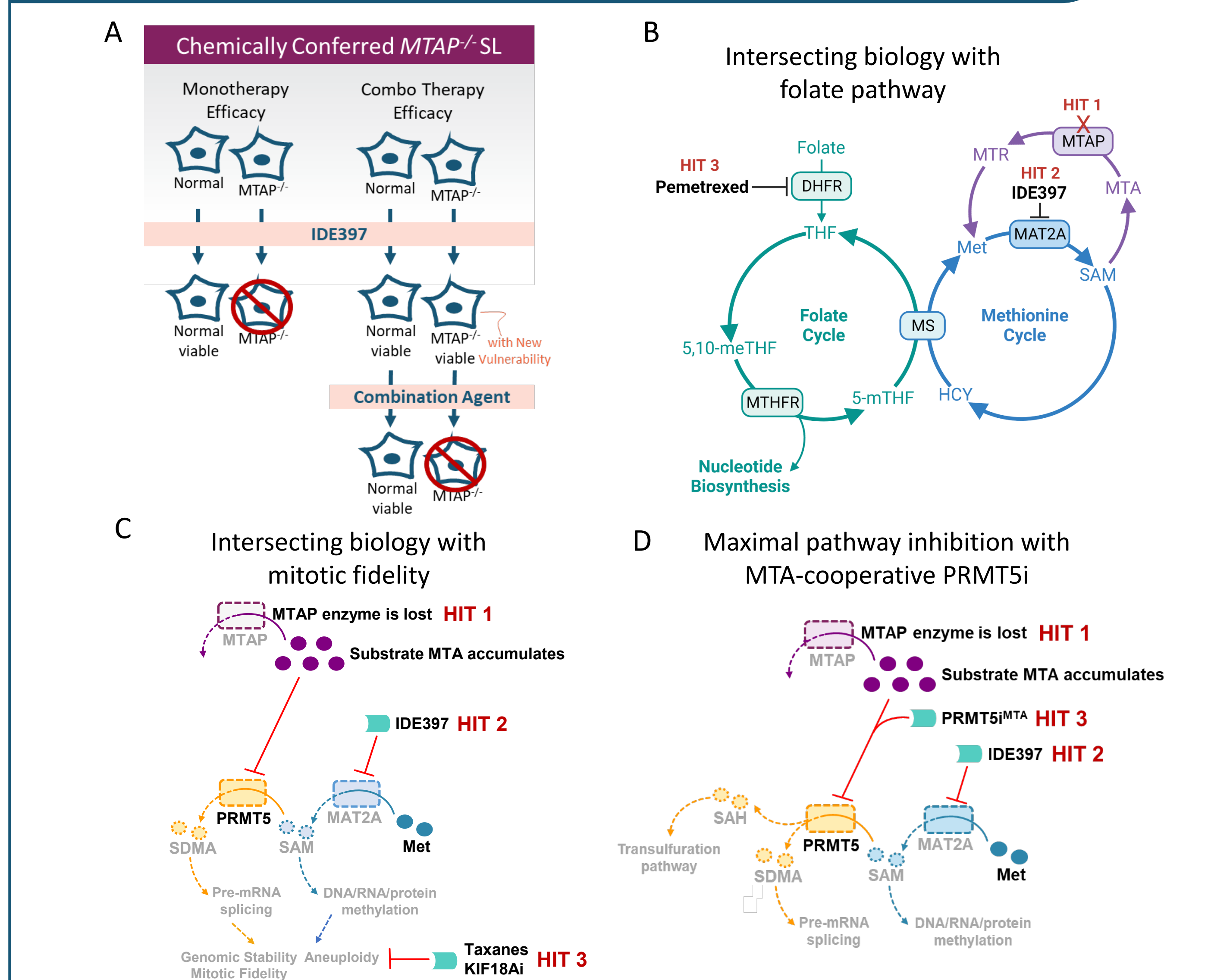
A) A PaCMAP dimensionality reduction generated from the cross-correlation between IDE397 and 1487 drugs in the DepMap PRISM repurposing dataset. IDE397 and correlates highlighted (orange). B) The IDE397-containing cluster from the 1488x1488 cross-correlation matrix (symmetric around the diagonal) showing IDE397 and its closest correlates. Highlighted drugs from panel A are colored by drug class (MOA). C) Individual Spearman correlation values between various drugs and IDE397, organized by target class.

Figure 6. Drug combination screens uncover synergistic interactions between IDE397 and perturbation of biological systems impacted by *MTAP* deficiency



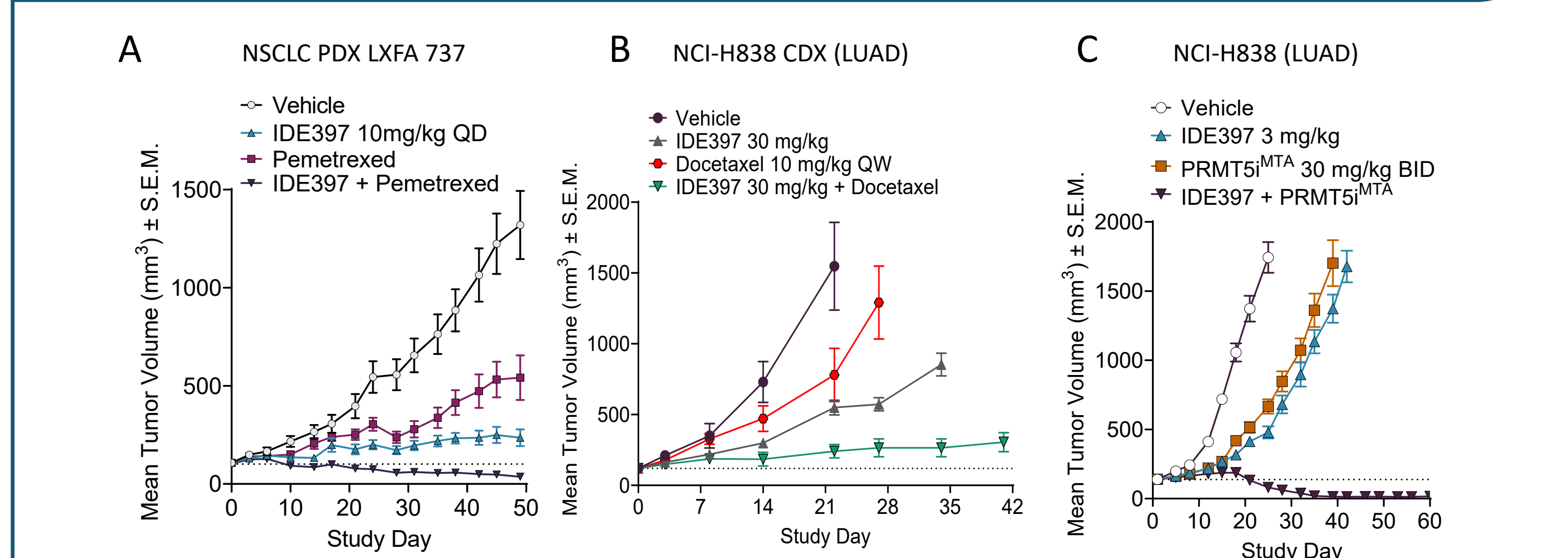
In vitro evaluation of IDE397 and multiple drug classes produce synergism in *MTAP*-deleted cell lines A) Collaborative study schematic B) IDE397 was screened with 101 drug partners in 13 *MTAP*-deleted cell lines in a 6x6 optimized dose matrix for 6 days. Heatmap indicates combinations that provided synergy as assessed by the Loewe model. Red shaded boxes indicate synergy, while gray boxes indicate no synergy. C) IDE397 was screened in a second study with 420 drug partners in 15 *MTAP*-WT and *MTAP*-deleted cell lines for 10 days. Table indicates top synergistic combinations (Bliss model) from follow-up studies using 8 *MTAP*-deleted cell lines. D) Examples of Bliss synergy (top panels) and growth death index (bottom panels) matrices for 16-point titrations of pemetrexed (x axis) and IDE397 (y axis) in *MTAP*-deleted NCI-H838 and UMCUC9 cell lines. Cells were either co-treated for 10 days (NCI-H838) or 4-day IDE397 pre-treatment then 6-day co-treatment (UMCUC9). E) Dose-response curves of IDE397 and combination partners. IDE397 and SPLAM or KIF18A combinations utilized co-treatment of 1 μM IDE397 and 20-point titration of SPLAM or KIF18A for 10 days. F) Dose response similar to E, but with fixed 1:1 ratio of inhibitor.

Figure 7. IDE397 combination therapies offer a paradigm for chemically conferred synthetic lethality in *MTAP*-deleted tumors



MAT2A inhibition may elicit new vulnerabilities in *MTAP*-deleted tumors that enable combination therapies. A) Model of chemically conferred synthetic lethality (SL) in *MTAP*-deleted tumors. MAT2A inhibition may sensitize *MTAP*-deleted tumors to B) pemetrexed-mediated impaired nucleotide biosynthesis due to the intersection of the methionine cycle and folate cycles, C) anti-mitotic agents due to the importance of MAT2A in maintaining mitotic fidelity, D) MTA-cooperative PRMT5i inhibitors (PRMT5i^{MTA}) through maximal pathway inhibition.

Figure 8. Combination of IDE397 with anti-folates, taxanes, or MTA-cooperative PRMT5i provides enhanced anti-tumor activity



Combination of IDE397 and either pemetrexed, paclitaxel, or MTA-cooperative PRMT5i inhibitor (PRMT5i^{MTA}) provides enhanced anti-tumor efficacy in *MTAP*-deleted xenograft models. A) Administration of 10 mg/kg QD PO IDE397 and 25 mg/kg 5 days on/2 days off IP pemetrexed produced tumor regressions in the NSCLC adenocarcinoma PDX model LXFA 737 (n=10/gp). B) Administration of 30 mg/kg QD PO IDE397 and 10 mg/kg QW IP docetaxel in NSCLC CDX model NCI-H838 (n=8 /gp). C) Administration of 3 mg/kg QD PO IDE397 and 30 mg/kg BID PO PRMT5i^{MTA} produced complete tumor regressions (n=10/gp).